





## Relativistic Stark energies of hydrogenlike ions

I. A. Maltsev <sup>1</sup>, D. A. Tumakov <sup>1</sup>, R. V. Popov <sup>2,1</sup> and V. M. Shabaev <sup>1,2</sup>

<sup>1</sup>*Department of Physics, St. Petersburg State University, Universitetskaya Naberezhnaya 7/9, 199034 St. Petersburg, Russia*

<sup>2</sup>*Petersburg Nuclear Physics Institute named by B. P. Konstantinov of National Research Centre “Kurchatov Institute”, Gatchina, Leningrad District 188300, Russia*



(Received 15 May 2023; revised 24 September 2023; accepted 26 September 2023; published 18 October 2023)

The relativistic energies and widths of hydrogenlike ions exposed to the uniform electric field are calculated. The calculations are performed for the ground and lowest excited states using the complex-scaling technique in combination with a finite-basis method. The obtained results are compared with the nonrelativistic values. The role of relativistic effects is investigated.

DOI: [10.1103/PhysRevA.108.042813](https://doi.org/10.1103/PhysRevA.108.042813)

### I. INTRODUCTION

The bound states of an atom placed in a uniform electric field are shifted and turn into resonances. The resonance states are embedded into the continuum and have finite energy width. This means that the atomic electrons can escape via tunneling through the potential barrier formed by the Coulomb and uniform electric fields. This phenomenon is referred to as a Stark effect and for many years has been studied in atomic systems experimentally [1–6] as well as theoretically [7–30]. Many theoretical approaches have been applied for calculation of Stark resonances. However, almost all of these calculations were nonrelativistic. The relativistic effects can have some impact even in light systems (see Ref. [22]). The relativistic treatment is required for searching for parity-nonconserving effects and physics beyond the standard model in molecules, where the Stark shifts play an important role (see, e.g., Refs. [31,32]). For heavy ions the relativistic consideration is absolutely necessary. Meanwhile, experiments with heavy partially stripped ions (PSIs) in very strong electric fields will soon become feasible.

One of the new projects, proposed currently as a part of the Physics Beyond Colliders initiative, is the Gamma Factory [33]. The proposed idea is to combine the relativistic beams of heavy PSIs at the Large Hadron Collider with the laser facility and use the Doppler boosting of the laser photons in the PSI reference frame. The PSI spectroscopy in strong external fields is one of the promising research topics of the project. If the PSI beam is placed in the transverse magnetic field, then in the PSI rest frame there exists an electric field enhanced by the  $\gamma$  factor. Modern high-field magnets allow generation of electric fields in the PSI rest frame of strength up to  $10^{12}$  V/cm or even higher [33]. A field of such strength allows manipulating the energy levels of heavy PSIs. The theoretical values of resonance positions seem to be highly required for such investigations. The values of the Stark widths are also important for estimation of ion beam stability, since ion losses due the Stark ionization of PSIs can take place.

For relatively weak fields the positions of the Stark resonances can be calculated using the relativistic perturbation theory [8,28]. In Ref. [28], the relativistic resonance positions were also obtained via numerically solving the Dirac

equation in a finite basis set, which allows us to take into account the external field exactly. However, since the resonance wave functions are not square integrable, the standard Hermite finite-basis-set methods cannot provide accurate values of the resonance positions [34]. Moreover, they cannot be directly used for calculation of the resonance widths. The relativistic values of the resonance widths were obtained in Refs. [23–25] using the semiclassical approximation. The semiclassical approach allows us to obtain the corresponding analytical expressions, but its accuracy is limited.

The precise values of the resonance positions as well as the resonance widths can be calculated with the complex-scaling (CS) method. The CS technique is based on dilation of the Hamiltonian into the complex plane. After the dilation the resonances appear as square-integrable solutions of the Dirac equation. The corresponding energies have complex values. The real part of the complex energy matches the resonance position and the imaginary part defines the resonance width. Previously, the CS method was successfully employed for relativistic calculations of many-electron autoionization states [34–37] and supercritical resonance in heavy quasimolecules [38–41]. Recently, the CS method was implemented in the Q-CHEM quantum chemistry program package, which is also able to take into account some relativistic effects [42,43]. A detailed description of the complex-scaling approach and its applications can be found in reviews in [44–48].

The relativistic CS method was used previously for calculations of Stark energies and widths of one-electron atomic systems in Refs. [22,30]. However, the calculations were restricted to only hydrogen and hydrogenlike neon. It should be noted that the Stark energies and widths for a hydrogenlike ion with the nuclear charge  $Z$  exposed to an electric field  $F$  can be easily obtained from the corresponding hydrogen values calculated for the field strength  $F/Z^3$  by multiplying them by  $Z^2$ . This scaling law is a direct consequence of the Schrödinger equation with a pointlike nucleus and there is no such rule for the relativistic case. Therefore, the relativistic calculations should be performed for every  $Z$  under consideration. Taking into account the finite nuclear size also breaks the scaling law.

The aim of the present work is to fill the gap in theoretical data and investigate the influence of the relativistic effects on

the Stark resonances. In order to achieve this aim we have performed calculations of the lowest resonance states for several hydrogenlike ions between  $Z = 1$  and 82. The resonance parameters are obtained utilizing the relativistic CS technique. After the complex scaling, the Dirac equation is solved using the finite-basis method described in Refs. [49,50]. The obtained results are compared with available nonrelativistic and relativistic values and the influence of the relativistic effects is investigated.

Throughout the paper we assume  $\hbar = 1$ .

## II. THEORY

The relativistic energy spectrum of a hydrogenlike ion is determined by the Dirac equation

$$H\psi(\mathbf{r}) = E\psi(\mathbf{r}), \quad (1)$$

where, in the presence of an external uniform electric field, the Hamiltonian has the following form:

$$H = c(\boldsymbol{\alpha} \cdot \mathbf{p}) + V_{\text{nucl}}(r) + eFz + \beta m_e c^2. \quad (2)$$

Here  $e$  is the electron charge ( $e = |e|$ ),  $V_{\text{nucl}}(r)$  is the nuclear potential, and  $F$  is the strength of the electric field, which is assumed to be directed along the  $z$  axis. For the nuclear potential, the pointlike nuclear model [ $V_{\text{nucl}}(r) = -eZ/r$ ] is generally used. However, in many cases, especially for heavy ions, the finite-nuclear-size effect is rather significant. Therefore, in the present work we utilize the model of a uniformly charged sphere, which takes into account the finite nuclear size

$$V_{\text{nucl}}(r) = \begin{cases} -\frac{eZ}{2R_{\text{nucl}}}\left(3 - \frac{r^2}{R_{\text{nucl}}^2}\right), & r < R_{\text{nucl}} \\ -\frac{eZ}{r}, & r > R_{\text{nucl}}, \end{cases} \quad (3)$$

where  $R_{\text{nucl}} = \sqrt{5/3}R_{\text{rms}}$  is the nuclear radius and  $R_{\text{rms}}$  is the root-mean-square nuclear radius.

The Dirac equation is considered in the spherical coordinate system  $(r, \theta, \varphi)$ . The Hamiltonian (2) is invariant under rotation around the  $z$  axis. Therefore, it is possible to separate the azimuthal angle  $\varphi$  from other coordinates. The separation can be done by substitution of the function

$$\psi_m(r, \theta, \varphi) = \frac{1}{r} \begin{pmatrix} G_1(r, \theta) \exp\left[i\left(m - \frac{1}{2}\right)\varphi\right] \\ G_2(r, \theta) \exp\left[i\left(m + \frac{1}{2}\right)\varphi\right] \\ iF_1(r, \theta) \exp\left[i\left(m - \frac{1}{2}\right)\varphi\right] \\ iF_2(r, \theta) \exp\left[i\left(m + \frac{1}{2}\right)\varphi\right] \end{pmatrix} \quad (4)$$

into the Dirac equation (1). Here  $m$  is the half-integer  $z$  projection of the total angular momentum. With this substitution, Eq. (1) can be reduced to the following form:

$$H_m \Phi(r, \theta) = E \Phi(r, \theta). \quad (5)$$

Here the four-component wave function  $\Phi(r, \theta)$  is given by

$$\Phi(r, \theta) = \begin{pmatrix} G_1(r, \theta) \\ G_2(r, \theta) \\ F_1(r, \theta) \\ F_2(r, \theta) \end{pmatrix} \quad (6)$$

and the Hamiltonian  $H_m$  can be represented as

$$H_m(t) = \begin{pmatrix} m_e c^2 + V_{\text{nucl}}(r) + eFz & cD_m \\ -cD_m & -m_e c^2 + V_{\text{nucl}}(r) + eFz \end{pmatrix}, \quad (7)$$

$$D_m = (\sigma_z \cos \theta + \sigma_x \sin \theta) \left( \frac{\partial}{\partial r} - \frac{1}{r} \right) + \frac{1}{r} (\sigma_x \cos \theta - \sigma_z \sin \theta) \frac{\partial}{\partial \theta} + \frac{1}{r \sin \theta} \left( im\sigma_y + \frac{1}{2}\sigma_x \right), \quad (8)$$

where  $\sigma_x$ ,  $\sigma_y$ , and  $\sigma_z$  are the Pauli matrices.

Due to the presence of the uniform field  $F$ , Eqs. (1) and (5) have no bound states. For nonzero  $F$  the original (at  $F = 0$ ) bound states of a hydrogenlike ion become embedded in the positive continuum and can be described as resonances. The resonances have finite energy widths  $\Gamma$ , which correspond to the probability of the electron being ionized via escaping through the potential barrier. In order to obtain the resonance positions and widths, we used the CS method. The simplest version of the CS technique is the uniform complex rotation, according to which the radial coordinate is transformed as  $r \rightarrow r e^{i\Theta}$ , where  $\Theta$  is a constant angle of the complex rotation. For the potential of a pointlike nucleus this transformation causes no problem and can be easily performed. However, if the potential is not an analytic function, then the uniform complex rotation cannot be done. In particular, the potential of the uniformly charged sphere given by Eq. (3) is not analytic. In order to overcome this obstacle, one can use the exterior complex scaling (ECS) proposed in Ref. [51]:

$$r \rightarrow \begin{cases} r, & r \leq r_0 \\ r_0 + (r - r_0)e^{i\Theta}, & r > r_0. \end{cases} \quad (9)$$

By such a transformation the internal region  $r \leq r_0$  remains untouched while the complex rotation is performed in the external region, where the potential is analytic. The drawback, however, is that after the substitution (9) the derivative of the Hamiltonian eigenfunction is discontinuous at  $r = r_0$ . Therefore, in order to get a correct finite-basis representation of the Dirac equation, one should use the basis functions which are also discontinuous at this point. Instead, in the present work we use a more universal version of the CS technique, namely, the smooth exterior complex scaling [47,52], which is defined by the transformation

$$r \rightarrow \begin{cases} r, & r \leq r_0 \\ r + (r - r_0)(e^{i\Theta} - 1)f(r), & r > r_0, \end{cases} \quad (10)$$

where the function  $f(r)$  is chosen as

$$f(r) = 1 - e^{-[(r-r_0)/a]^2}. \quad (11)$$

This transformation defines a smooth transition from  $r$  to  $r e^{i\Theta}$  for  $r \rightarrow \infty$ . It worth mentioning that there also exists a complex absorbing potential approach, which is quite close to the smooth ECS method [53]. A similar complex-scaling contour  $f(r)$  was used in Ref. [54]. The parameters  $r_0$  and  $a$

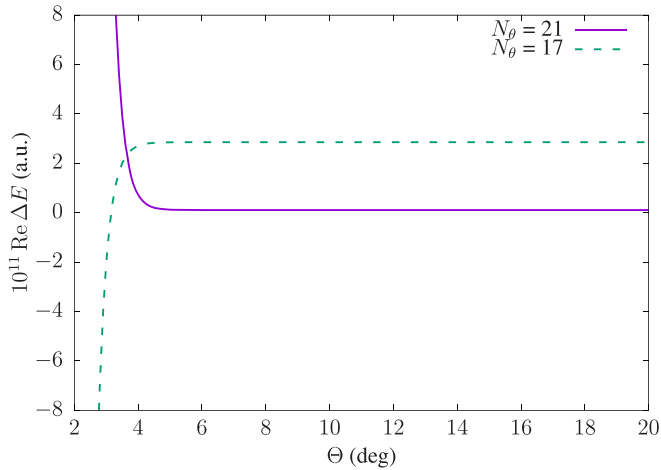


FIG. 1. Real part of the complex Stark energy  $E$  as a function of the complex-scaling angle  $\Theta$  for a hydrogen atom exposed to an electric field of strength  $F = 0.05$  a.u. Here  $\Delta E = E - E_0$ , where  $\text{Re } E_0 = -0.5061117144$  a.u. The solid line corresponds to the results obtained using the basis set with  $N_\theta = 21$  and the dashed line corresponds to the values obtained with  $N_\theta = 17$ .

can be adjusted in order to facilitate the convergence of the numerical calculation. The smooth ECS is more flexible than the sharp one defined by Eq. (9). It should be noted, however, that, at least in some cases, the sharp ECS can provide more stable results than its smooth counterpart [55].

After the transformation (9) or (10) the Stark resonances match the square-integrable solutions of Eq. (5) and the corresponding energy  $E$  has a complex value

$$E = E_0 - i\Gamma/2. \quad (12)$$

The real part  $E_0$  is the position of the resonance and the imaginary part defines the resonance width  $\Gamma$ .

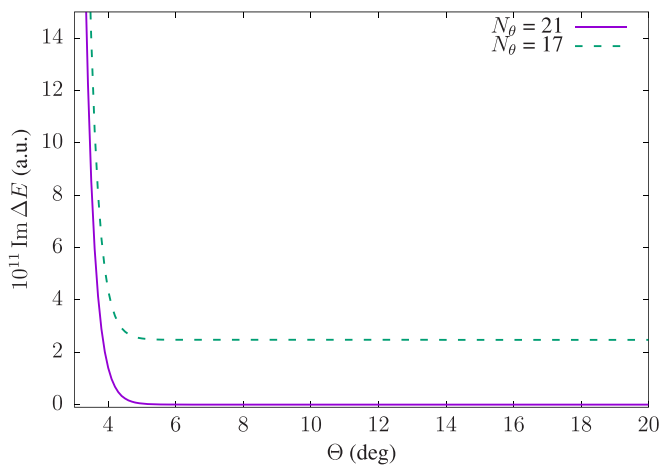


FIG. 2. Imaginary part of the complex Stark energy  $E$  as a function of the complex-scaling angle  $\Theta$  for a hydrogen atom exposed to an electric field of strength  $F = 0.05$  a.u. Here  $\Delta E = E - E_0$ , where  $\text{Im } E_0 = -3.85812927 \times 10^{-5}$  a.u. The solid line corresponds to the results obtained using the basis set with  $N_\theta = 21$  and the dashed line corresponds to the values obtained with  $N_\theta = 17$ .

TABLE I. Real  $E$  and imaginary  $-\Gamma/2$  parts of the complex energy of a hydrogen atom exposed to a uniform electric field  $F = 0.05$  a.u. The calculations were performed with the basis set constructed using  $N_r$  radial and  $N_\theta$  angular  $B$  splines.

$N_\theta$	$E$ (a.u.)		$-\Gamma/2 \times 10^5$ (a.u.)	
	$N_r = 300$	$N_r = 500$	$N_r = 300$	$N_r = 500$
11	-0.50611708053	-0.50611708062	-3.85792525	-3.85792458
13	-0.50611714238	-0.50611714243	-3.85812570	-3.85812576
15	-0.50611714322	-0.50611714327	-3.85812084	-3.85812085
17	-0.50611714365	-0.50611714371	-3.85812676	-3.85812680
19	-0.50611714385	-0.50611714390	-3.85812856	-3.85812859
21	-0.50611714393	-0.50611714398	-3.85812923	-3.85812927

TABLE II. Stark shifts  $\Delta E$  and widths  $\Gamma$  of the ground-state resonance of hydrogenlike ions with the nuclear charge  $Z$  as functions of the field strength  $F$ . The relativistic results were obtained in this work. The nonrelativistic results are the hydrogen values from Ref. [9] multiplied by  $Z^2$ .

$F/Z^3$ (a.u.)	Relativistic		Nonrelativistic	
	$\Delta E$ (a.u.)	$-\Gamma/2$ (a.u.)	$\Delta E$ (a.u.)	$-\Gamma/2$ (a.u.)
		$Z = 1, R_{\text{rms}} = 0.8775 \text{ fm}$		
0.03	$-2.0741555(1) \times 10^{-3}$	$-1.11825(2) \times 10^{-8}$	$-2.074273 \times 10^{-3}$	$-1.11880 \times 10^{-8}$
0.04	$-3.7713727(1) \times 10^{-3}$	$-1.945666(6) \times 10^{-6}$	$-3.771591 \times 10^{-3}$	$-1.94635 \times 10^{-6}$
0.05	$-6.1050580(1) \times 10^{-3}$	$-3.858129(5) \times 10^{-5}$	$-6.105425 \times 10^{-3}$	$-3.859208 \times 10^{-5}$
0.06	$-9.2028811(1) \times 10^{-3}$	$-2.574804(1) \times 10^{-4}$	$-9.203451 \times 10^{-3}$	$-2.5753874 \times 10^{-4}$
0.07	$-1.30759641(1) \times 10^{-2}$	$-9.235128(2) \times 10^{-4}$	$-1.307677 \times 10^{-2}$	$-9.2368428 \times 10^{-4}$
0.08	$-1.75595902(1) \times 10^{-2}$	$-2.2694781(2) \times 10^{-3}$	$-1.756062 \times 10^{-2}$	$-2.2698288 \times 10^{-3}$
0.09	$-2.24115841(2) \times 10^{-2}$	$-4.3914109(4) \times 10^{-3}$	$-2.241281 \times 10^{-2}$	$-4.3919872 \times 10^{-3}$
0.1	$-2.74167896(5) \times 10^{-2}$	$-7.2682294(4) \times 10^{-3}$	$-2.741818 \times 10^{-2}$	$-7.2690568 \times 10^{-3}$
		$Z = 10, R_{\text{rms}} = 3.0055 \text{ fm}$		
0.03	$-2.0625762(1) \times 10^{-1}$	$-1.06837(2) \times 10^{-6}$	$-2.074273 \times 10^{-1}$	$-1.11880 \times 10^{-6}$
0.04	$-3.7497908(1) \times 10^{-1}$	$-1.879052(6) \times 10^{-4}$	$-3.771591 \times 10^{-1}$	$-1.94635 \times 10^{-4}$
0.05	$-6.0687382(1) \times 10^{-1}$	$-3.752554(5) \times 10^{-3}$	$-6.105425 \times 10^{-1}$	$-3.859208 \times 10^{-3}$
0.06	$-9.1465468(1) \times 10^{-1}$	$-2.517546(1) \times 10^{-2}$	$-9.203451 \times 10^{-1}$	$-2.5753874 \times 10^{-2}$
0.07	$-1.29966685(1)$	$-9.066438(2) \times 10^{-2}$	$-1.307677$	$-9.2368428 \times 10^{-2}$
0.08	$-1.74579789(1)$	$-2.2349116(2) \times 10^{-1}$	$-1.756062$	$-2.2698288 \times 10^{-1}$
0.09	$-2.22904989(2)$	$-4.3345338(3) \times 10^{-1}$	$-2.241281$	$-4.3919872 \times 10^{-1}$
0.1	$-2.72795663(5)$	$-7.1865027(4) \times 10^{-1}$	$-2.741818$	$-7.2690568 \times 10^{-1}$
		$Z = 18, R_{\text{rms}} = 3.4028 \text{ fm}$		
0.03	$-6.598073(1) \times 10^{-1}$	$-3.11911(7) \times 10^{-6}$	$-6.720643 \times 10^{-1}$	$-3.62491 \times 10^{-6}$
0.04	$-1.1991590(1)$	$-5.62253(2) \times 10^{-4}$	$-1.221995$	$-6.30617 \times 10^{-4}$
0.05	$-1.9397447(1)$	$-1.141133(2) \times 10^{-2}$	$-1.978158$	$-1.250383 \times 10^{-2}$
0.06	$-2.9223297(1)$	$-7.747931(4) \times 10^{-2}$	$-2.981918$	$-8.3442552 \times 10^{-2}$
0.07	$-4.1529243(1)$	$-2.8161645(6) \times 10^{-1}$	$-4.236872$	$-2.9927371 \times 10^{-1}$
0.08	$-5.5819469(1)$	$-6.9910647(8) \times 10^{-1}$	$-5.689640$	$-7.3542452 \times 10^{-1}$
0.09	$-7.1332880(1)$	$-1.3630835(1)$	$-7.261750$	$-1.4230039$
0.1	$-8.7377925(2)$	$-2.2689107(1)$	$-8.883489$	$-2.3551744$
		$Z = 36, R_{\text{rms}} = 4.1835 \text{ fm}$		
0.03	$-2.4936111(1)$	$-7.8166(3) \times 10^{-6}$	$-2.688257$	$-1.44996 \times 10^{-5}$
0.04	$-4.5259171(1)$	$-1.572824(6) \times 10^{-3}$	$-4.887982$	$-2.52247 \times 10^{-3}$
0.05	$-7.3048551(1)$	$-3.430401(5) \times 10^{-2}$	$-7.912631$	$-5.001534 \times 10^{-2}$
0.06	$-1.09845515(1) \times 10^1$	$-2.456480(2) \times 10^{-1}$	$-1.192767 \times 10^1$	$-3.3377021 \times 10^{-1}$
0.07	$-1.56140755(1) \times 10^1$	$-9.304429(2) \times 10^{-1}$	$-1.694749 \times 10^1$	$-1.1970948$
0.08	$-2.10396505(1) \times 10^1$	$-2.3841355(3)$	$-2.275856 \times 10^1$	$-2.9416981$
0.09	$-2.69874032(2) \times 10^1$	$-4.7610474(4)$	$-2.904700 \times 10^1$	$-5.6920155$
0.1	$-3.31897931(5) \times 10^1$	$-8.0689585(6)$	$-3.553395 \times 10^1$	$-9.4206976$
		$Z = 54, R_{\text{rms}} = 4.7964 \text{ fm}$		
0.03	$-5.075628(1)$	$-7.5824(6) \times 10^{-6}$	$-6.048579$	$-3.26242 \times 10^{-5}$
0.04	$-9.192809(1)$	$-1.856289(8) \times 10^{-3}$	$-1.099796 \times 10^1$	$-5.67556 \times 10^{-3}$
0.05	$-1.4783894(1) \times 10^1$	$-4.599133(8) \times 10^{-2}$	$-1.780342 \times 10^1$	$-1.125345 \times 10^{-1}$
0.06	$-2.2152360(1) \times 10^1$	$-3.617239(3) \times 10^{-1}$	$-2.683726 \times 10^1$	$-7.5098297 \times 10^{-1}$
0.07	$-3.1473089(1) \times 10^1$	$-1.4738926(5)$	$-3.813185 \times 10^1$	$-2.6934634$
0.08	$-4.2554122(1) \times 10^1$	$-3.9978229(6)$	$-5.120676 \times 10^1$	$-6.6188207$
0.09	$-5.4907367(1) \times 10^1$	$-8.3398840(8)$	$-6.535575 \times 10^1$	$-1.2807035 \times 10^1$
0.1	$-6.7983841(1) \times 10^1$	$-1.4612320(1) \times 10^1$	$-7.995140 \times 10^1$	$-2.1196570 \times 10^1$
		$Z = 82, R_{\text{rms}} = 5.5012 \text{ fm}$		
0.03	$-8.935694(1)$	$-1.646(1) \times 10^{-6}$	$-1.394741 \times 10^1$	$-7.52281 \times 10^{-5}$
0.04	$-1.6112143(1) \times 10^1$	$-6.92395(5) \times 10^{-4}$	$-2.536018 \times 10^1$	$-1.30873 \times 10^{-2}$
0.05	$-2.5712020(1) \times 10^1$	$-2.427590(6) \times 10^{-2}$	$-4.105288 \times 10^1$	$-2.594931 \times 10^{-1}$
0.06	$-3.8160498(1) \times 10^1$	$-2.455934(3) \times 10^{-1}$	$-6.188400 \times 10^1$	$-1.7316905$
0.07	$-5.3920546(1) \times 10^1$	$-1.2177878(7)$	$-8.792817 \times 10^1$	$-6.2108531$
0.08	$-7.3126730(1) \times 10^1$	$-3.863345(1)$	$-1.180776 \times 10^2$	$-1.5262329 \times 10^1$
0.09	$-9.5381168(1) \times 10^1$	$-9.125540(1)$	$-1.507037 \times 10^2$	$-2.9531722 \times 10^1$
0.1	$-1.19906312(1) \times 10^2$	$-1.7627242(2) \times 10^1$	$-1.843598 \times 10^2$	$-4.8877138 \times 10^1$

The complex-rotated Dirac equation is solved using the finite-basis method. The wave function  $\Phi(r, \theta)$  [see Eq. (4)] is expanded as

$$\Phi(r, \theta) = \sum_{n=1}^N C_n W_n(r, \theta). \quad (13)$$

The basis functions  $W_n(r, \theta)$  are constructed from  $N_\theta$ ,  $B$  splines dependent on the  $\theta$  coordinate and  $N_r$ ,  $B$  splines dependent on the  $r$  coordinate. The total number of basis functions is  $N = 4 \times N_r \times N_\theta$ . The construction is performed using the dual-kinetic balance technique for axially symmetric systems. This technique prevents the appearance of spurious states in the spectrum. A detailed description of the employed basis set can be found in Ref. [49]. By the substitution of Eq. (13), the Dirac equation (5) is reduced to the generalized eigenvalue problem

$$\sum_{k=1}^N H_{jk} C_k = \sum_{k=1}^N E S_{jk} C_k. \quad (14)$$

Here  $H_{jk}$  and  $S_{jk}$  correspond to the Hamiltonian and overlap matrices, respectively. The complex eigenvalues  $E$  are found using the numerical diagonalization procedure.

### III. RESULTS AND DISCUSSION

In the present work, only states with the projection of total angular momentum  $m = 1/2$  are considered. The complex Stark energies are obtained by solving the eigenvalue problem (14). The resonance positions and widths are related to the complex eigenvalues via Eq. (12).

For each nuclear charge  $Z$  considered the basis set is constructed from the  $B$  splines defined in a box of size  $r_{\max} \approx 174/Z$  a.u. The radial  $B$ -spline knots are distributed uniformly inside the nucleus and exponentially outside. We use the smooth ECS technique with the contour defined by Eq. (11) with  $a = 7.75/Z$  a.u. The following values of the contour parameter  $r_0/Z$  are chosen depending on the electric-field strength  $F$  and the atomic state under consideration: 11, 8, and 5 for the ground state, with  $F/Z^3 \leq 0.04$ ,  $0.04 < F/Z^3 \leq 0.07$ , and  $F/Z^3 > 0.07$ , respectively, and 5 for all excited states (all quantities are given in atomic units). By adjusting the values of  $r_0$  and  $a$  it is possible to improve the stability and convergence of the energy values. Note, however, that accurate results can be obtained with a quite broad range of these parameters.

The exact solutions of the complex-scaled Dirac equation corresponding to the resonances do not depend on the angle of complex scaling  $\Theta$ . However, the solutions of the finite-basis representation (14) exhibit such a dependence. In our case, the rapid change in the real and imaginary parts of the complex energy  $E$  for small values of  $\Theta$  is followed by a long plateau (see Figs. 1 and 2 for the real and imaginary parts, respectively). Despite the fact that the energy values are not perfectly stable on the plateau, as can be seen from Figs. 1 and 2, the dependence on  $\Theta$  is much smaller than the difference between the values obtained with the basis sets of close sizes. This shows that the  $\Theta$  dependence is negligible in comparison with the uncertainty which comes from the basis convergence.

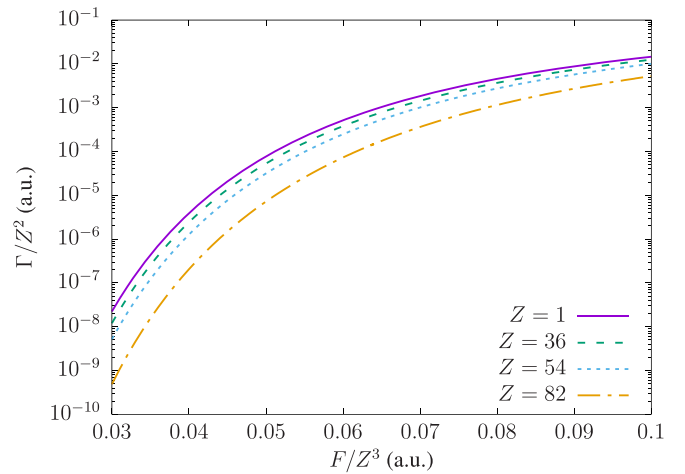


FIG. 3. Relativistic Stark width  $\Gamma$  of the ground state of the hydrogenlike ion with nuclear charge  $Z$  in the presence of a uniform electric field  $F$ . In the nonrelativistic limit, the values for all  $Z$  should be the same. The difference is caused by the relativistic effects.

The calculations are performed using the basis sets of different sizes for a wide range of CS angle  $\Theta$ . As an example, in Table I we present the results for a hydrogen atom exposed to an electric field  $F = 0.05$  a.u., which are obtained utilizing different numbers of radial and angular  $B$  splines ( $N_r$  and  $N_\theta$ , respectively). The largest employed basis set has the following parameters:  $N_r = 500$  and  $N_\theta = 21$  with the total number of the basis functions  $N = 40\,000$ . The calculational uncertainty is estimated from the convergence of the results. The estimation is done in such a way that the estimated uncertainty is well above the difference between the value for the largest basis set and any reasonable interpolation of the results to the complete-basis-set limit.

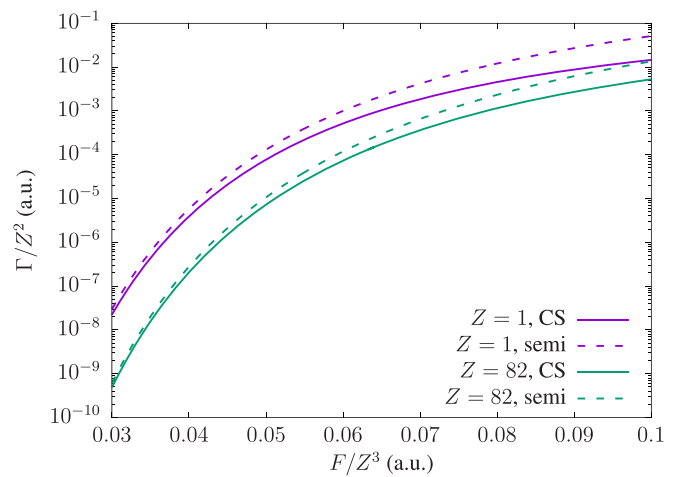


FIG. 4. Relativistic Stark width  $\Gamma$  for the ground state of the hydrogenlike ion with nuclear charge  $Z$  in the presence of a uniform electric field  $F$ . Solid lines show the results obtained with the complex-scaling methods and dashed lines the values calculated using the semiclassical theory. The upper curves correspond to  $Z = 1$  and the lower ones correspond to  $Z = 82$ .

TABLE III. Stark shifts  $\Delta E$  and widths  $\Gamma$  of the  $2p_{1/2}$  resonance of hydrogenlike ions with the nuclear charge  $Z$  as functions of the field strength  $F$ . The relativistic results were obtained in this work. The nonrelativistic results are the hydrogen values from Ref. [19] multiplied by  $Z^2$ .

$F/Z^3$ (a.u.)	Relativistic		Nonrelativistic	
	$\Delta E$ (a.u.)	$-\Gamma/2$ (a.u.)	$\Delta E$ (a.u.)	$-\Gamma/2$ (a.u.)
		$Z = 1, R_{\text{rms}} = 0.8775$ fm		
0.005	$-1.76176897(8) \times 10^{-2}$	$-5.29586(3) \times 10^{-5}$	$-1.761861 \times 10^{-2}$	$-5.2972236 \times 10^{-5}$
0.01	$-4.10926693(5) \times 10^{-2}$	$-5.442161(2) \times 10^{-3}$	$-4.109400 \times 10^{-2}$	$-5.4425560 \times 10^{-3}$
0.02	$-8.1680516(7) \times 10^{-2}$	$-3.0391832(5) \times 10^{-2}$	$-8.182220 \times 10^{-2}$	$-3.0392847 \times 10^{-2}$
0.03	$-1.1514503(2) \times 10^{-1}$	$-5.981855(6) \times 10^{-2}$	$-1.151471 \times 10^{-1}$	$-5.982000 \times 10^{-2}$
		$Z = 10, R_{\text{rms}} = 3.0055$ fm		
0.005	$-1.75268320(8)$	$-5.16194(3) \times 10^{-3}$	$-1.761861$	$-5.2972236 \times 10^{-3}$
0.01	$-4.09605836(5)$	$-5.403122(2) \times 10^{-1}$	$-4.109400$	$-5.4425560 \times 10^{-1}$
0.02	$-8.1509830(7)$	$-3.0290352(5)$	$-8.182220$	$-3.0392847$
0.03	$-1.1493599(2) \times 10^1$	$-5.966553(6)$	$-1.151471 \times 10^1$	$-5.982000$
		$Z = 18, R_{\text{rms}} = 3.4028$ fm		
0.005	$-5.6121159(3)$	$-1.576507(8) \times 10^{-2}$	$-5.708429$	$-1.7163004 \times 10^{-2}$
0.01	$-1.31737804(2) \times 10^1$	$-1.7218961(6)$	$-1.331446 \times 10^1$	$-1.7633881$
0.02	$-2.6283190(2) \times 10^1$	$-9.739293(2)$	$-2.651039 \times 10^1$	$-9.8472823$
0.03	$-3.7085071(6) \times 10^1$	$-1.921889(2) \times 10^1$	$-3.730767 \times 10^1$	$-1.938168 \times 10^1$
		$Z = 36, R_{\text{rms}} = 4.1835$ fm		
0.005	$-2.1296520(1) \times 10^1$	$-4.78561(3) \times 10^{-2}$	$-2.283372 \times 10^1$	$-6.8652017 \times 10^{-2}$
0.01	$-5.09632086(5) \times 10^1$	$-6.382976(2)$	$-5.325783 \times 10^1$	$-7.0535526$
0.02	$-1.02887904(7) \times 10^2$	$-3.7633130(6) \times 10^1$	$-1.060416 \times 10^2$	$-3.9389129 \times 10^1$
0.03	$-1.4560076(2) \times 10^2$	$-7.488076(7) \times 10^1$	$-1.492307 \times 10^2$	$-7.752672 \times 10^1$
		$Z = 54, R_{\text{rms}} = 4.7964$ fm		
0.005	$-4.3657867(2) \times 10^1$	$-6.26878(4) \times 10^{-2}$	$-5.137586 \times 10^1$	$-1.5446704 \times 10^{-1}$
0.01	$-1.078292818(7) \times 10^2$	$-1.2420509(5) \times 10^1$	$-1.198301 \times 10^2$	$-1.5870493 \times 10^1$
0.02	$-2.2256483(1) \times 10^2$	$-7.947587(1) \times 10^1$	$-2.385935 \times 10^2$	$-8.8625541 \times 10^1$
0.03	$-3.1676073(3) \times 10^2$	$-1.606622(1) \times 10^2$	$-3.357690 \times 10^2$	$-1.744351 \times 10^2$
		$Z = 82, R_{\text{rms}} = 5.5012$ fm		
0.005	$-7.8941197(3) \times 10^1$	$-2.35907(2) \times 10^{-2}$	$-1.184675 \times 10^2$	$-3.5618531 \times 10^{-1}$
0.01	$-2.07353215(1) \times 10^2$	$-1.773695(1) \times 10^1$	$-2.763161 \times 10^2$	$-3.6595747 \times 10^1$
0.02	$-4.5752851(1) \times 10^2$	$-1.5173717(2) \times 10^2$	$-5.501725 \times 10^2$	$-2.0436150 \times 10^2$
0.03	$-6.6341661(1) \times 10^2$	$-3.231929(2) \times 10^2$	$-7.742493 \times 10^2$	$-4.022297 \times 10^2$

In order to investigate the impact of the relativistic effects on the Stark resonances, we perform calculations for several hydrogenlike ions between  $Z = 1$  and 82. The obtained results are compared with the corresponding nonrelativistic values. The latter can be trivially obtained (in the pointlike nuclear model) for every  $Z$  from the hydrogen values using the scaling law  $F \rightarrow Z^3 F$ ,  $E_0 \rightarrow Z^2 E_0$ , and  $\Gamma \rightarrow Z^2 \Gamma$ , where  $F$  is the field strength and  $E_0$  and  $\Gamma$  are the resonance position and width, respectively. Here and below relativistic effects refer to the differences between the solutions of the Dirac and Schrödinger equations. They naturally include all the relativistic corrections (such as spin-orbit correction), which are usually used to improve the accuracy of nonrelativistic values. It should be noted, however, that in our calculations the finite nuclear model is utilized, while the scaled nonrelativistic values imply the pointlike nucleus. However, we found that the finite-nuclear-size contribution is relatively small and does not qualitatively affect the results.

The calculations are carried for the ground ( $1s$ ) and the lowest excited states ( $2s$ ,  $2p_{1/2}$ , and  $2p_{3/2}$ ). In the present work we classify the resonance states by the atomic states

with which they are coincident in the zero-field limit ( $F = 0$ ). In nonrelativistic studies of the Stark effect, another notation, which is based on parabolic quantum numbers ( $n_1, n_2, m_L$ ) [56], is usually used. For the states considered there is the following correspondence between the notations:  $1s$ ,  $2s$ ,  $2p_{1/2}$ , and  $2p_{3/2}$  match  $(0, 0, 0)$ ,  $(0, 1, 0)$ ,  $(0, 0, 1)$ , and  $(1, 0, 0)$ , respectively. The results obtained for the Stark shift  $\Delta E$  and Stark width  $\Gamma$  of the ground state and their nonrelativistic counterparts are presented in Table II. The nonrelativistic values for hydrogen are taken from Ref. [9] and those for  $Z \neq 1$  are derived via scaling of the hydrogen ones. As can be seen from the table, the relative difference between the relativistic and nonrelativistic Stark shift values is almost the same for all considered field strengths  $F$  and grows with  $Z$ . All the relativistic width values are smaller than the nonrelativistic ones, and the difference is larger for weaker fields and higher  $Z$ . For the lead ion ( $Z = 82$ ) for  $F \leq 0.04 \times Z^3$  the relativistic width value is suppressed relative to the nonrelativistic one by more than one order of magnitude.

In order to better illustrate the dependence of the relativistic effects on  $Z$  and  $F$ , we present the scaled width  $\Gamma/Z^2$

TABLE IV. Stark shifts  $\Delta E$  and widths  $\Gamma$  of the  $2s$  resonance of hydrogenlike ions with the nuclear charge  $Z$  as functions of the field strength  $F$ . The relativistic results were obtained in this work. The nonrelativistic results are the hydrogen values from Ref. [19] multiplied by  $Z^2$ .

$F/Z^3$ (a.u.)	Relativistic		Nonrelativistic	
	$\Delta E$ (a.u.)	$-\Gamma/2$ (a.u.)	$\Delta E$ (a.u.)	$-\Gamma/2$ (a.u.)
		$Z = 1, R_{\text{rms}} = 0.8775 \text{ fm}$		
0.005	$-2.145930(1) \times 10^{-3}$	$-1.30722(3) \times 10^{-5}$	$-2.146613 \times 10^{-3}$	$-1.3076437 \times 10^{-5}$
0.01	$-9.5239060(7) \times 10^{-3}$	$-3.138327(6) \times 10^{-3}$	$-9.524887 \times 10^{-3}$	$-3.1386570 \times 10^{-3}$
0.02	$-2.172828(4) \times 10^{-2}$	$-2.185255(6) \times 10^{-2}$	$-2.172946 \times 10^{-2}$	$-2.1853572 \times 10^{-2}$
0.03	$-2.83555(4) \times 10^{-2}$	$-4.44219(2) \times 10^{-2}$	$-2.835714 \times 10^{-2}$	$-4.4424040 \times 10^{-2}$
		$Z = 10, R_{\text{rms}} = 3.0055 \text{ fm}$		
0.005	$-2.078337(1) \times 10^{-1}$	$-1.26770(3) \times 10^{-3}$	$-2.146613 \times 10^{-1}$	$-1.3076437 \times 10^{-3}$
0.01	$-9.4265659(7) \times 10^{-1}$	$-3.106086(6) \times 10^{-1}$	$-9.524887 \times 10^{-1}$	$-3.1386570 \times 10^{-1}$
0.02	$-2.161869(4)$	$-2.174493(6)$	$-2.172946$	$-2.1853572$
0.03	$-2.82390(4)$	$-4.42479(2)$	$-2.835714$	$-4.4424040$
		$Z = 18, R_{\text{rms}} = 3.4028 \text{ fm}$		
0.005	$-6.236963(4) \times 10^{-1}$	$-3.85273(9) \times 10^{-3}$	$-6.955025 \times 10^{-1}$	$-4.2367655 \times 10^{-3}$
0.01	$-2.9824595(2)$	$-9.82897(2) \times 10^{-1}$	$-3.086063$	$-1.0169249$
0.02	$-6.92365(1)$	$-6.96632(2)$	$-7.040345$	$-7.0805573$
0.03	$-9.0636(1)$	$-1.420845(7) \times 10^1$	$-9.187712$	$-1.4393389 \times 10^1$
		$Z = 36, R_{\text{rms}} = 4.1835 \text{ fm}$		
0.005	$-1.625689(2)$	$-1.27550(3) \times 10^{-2}$	$-2.782010$	$-1.6947062 \times 10^{-2}$
0.01	$-1.06592307(2) \times 10^1$	$-3.534916(7)$	$-1.234425 \times 10^1$	$-4.0676994$
0.02	$-2.625980(4) \times 10^1$	$-2.648461(7) \times 10^1$	$-2.816138 \times 10^1$	$-2.8322229 \times 10^1$
0.03	$-3.47389(4) \times 10^1$	$-5.45927(2) \times 10^1$	$-3.675085 \times 10^1$	$-5.7573556 \times 10^1$
		$Z = 54, R_{\text{rms}} = 4.7964 \text{ fm}$		
0.005	$-3.94071(3) \times 10^{-1}$	$-2.53892(4) \times 10^{-2}$	$-6.259523$	$-3.8130889 \times 10^{-2}$
0.01	$-1.9015147(1) \times 10^1$	$-6.56114(1)$	$-2.777457 \times 10^1$	$-9.1523237$
0.02	$-5.341589(5) \times 10^1$	$-5.43389(1) \times 10^1$	$-6.336311 \times 10^1$	$-6.3725015 \times 10^1$
0.03	$-7.22343(8) \times 10^1$	$-1.142448(4) \times 10^2$	$-8.268941 \times 10^1$	$-1.2954050 \times 10^2$
		$Z = 82, R_{\text{rms}} = 5.5012 \text{ fm}$		
0.005	$1.4704343(5) \times 10^1$	$-2.44920(2) \times 10^{-2}$	$-1.443382 \times 10^1$	$-8.7925960 \times 10^{-2}$
0.01	$-1.5160798(8) \times 10^1$	$-8.80437(2)$	$-6.404534 \times 10^1$	$-2.1104329 \times 10^1$
0.02	$-8.8440982(6) \times 10^1$	$-9.59044(1) \times 10^1$	$-1.461089 \times 10^2$	$-1.4694342 \times 10^2$
0.03	$-1.30752(1) \times 10^2$	$-2.144554(3) \times 10^2$	$-1.906734 \times 10^2$	$-2.9870724 \times 10^2$

as a function of the scaled field strength  $F/Z^3$  for several  $Z$  in Fig. 3. In the nonrelativistic limit for the pointlike nuclei, all the curves should be the same. The difference is caused by the relativistic effects. As one can see from the figure, the divergence of the curves is larger for the weaker fields and this behavior becomes more pronounced for higher  $Z$ . The fact that the relativistic corrections have more impact for the weaker fields seems paradoxical. This phenomenon was discovered previously using the semiclassical approximation [23–25] and found to be a consequence of a relativistic increase of the binding energy. The CS results obtained for  $Z = 1$  and 82 are compared to the semiclassical ones in Fig. 4. The semiclassical values were calculated according to Eq. (36) from Ref. [24]. As one can see, the semiclassical theory indeed provides the qualitatively correct dependence of the width on the field strength. However, the semiclassical values are systematically larger than the CS ones and quantitatively valid only for small  $F$ . Such an overestimation of the width by the semiclassical approximation is already known in the nonrelativistic case (see, for example, Ref. [26]). The

confirmed relativistic suppression of the Stark width means that a heavy ion exposed to the electric field can be much more stable than the result obtained from the nonrelativistic calculations.

In Tables III–V we present the results for the excited  $2p_{1/2}$ ,  $2s$ , and  $2p_{3/2}$  states, respectively. As one can see from the tables, for  $2p_{1/2}$  and  $2s$  resonances the relativistic widths are also suppressed with respect to the nonrelativistic ones and the difference is larger for weaker field  $F$  and higher  $Z$ . The  $2p_{3/2}$  state, however, is a notable exception. For  $Z \geq 18$  and  $F/Z^3 = 0.05$  a.u. the relativistic width of  $2p_{3/2}$  state is larger than the nonrelativistic value and for  $Z = 82$  the difference is more than one order of magnitude. A possible explanation for such a drastic discrepancy is the influence of the spin-orbital interaction, which can play a significant role for small  $F$ . This suggests that this effect can be found using the two-component calculation methods. In the case of heavy ions, however, their accuracy is quite limited.

Almost all the presented relativistic values of the energy shift are slightly smaller than the nonrelativistic counter-

TABLE V. Stark shifts  $\Delta E$  and widths  $\Gamma$  of the  $2p_{3/2}$  resonance of hydrogenlike ions with the nuclear charge  $Z$  as functions of the field strength  $F$ . The relativistic results were obtained in this work. The nonrelativistic results are the hydrogen values from Ref. [19] multiplied by  $Z^2$ .

$F/Z^3$ (a.u.)	Relativistic		Nonrelativistic	
	$\Delta E$ (a.u.)	$-\Gamma/2$ (a.u.)	$\Delta E$ (a.u.)	$-\Gamma/2$ (a.u.)
		$Z = 1, R_{\text{rms}} = 0.8775$ fm		
0.005	$1.2936853(1) \times 10^{-2}$	$-2.8636(2) \times 10^6$	$1.293808 \times 10^{-2}$	$-2.864697 \times 10^6$
0.01	$2.1104324(3) \times 10^{-2}$	$-1.639384(7) \times 10^{-3}$	$2.110544 \times 10^{-2}$	$-1.6396395 \times 10^{-3}$
0.02	$3.60149(4) \times 10^{-2}$	$-1.54447(3) \times 10^{-2}$	$3.601573 \times 10^{-2}$	$-1.5446311 \times 10^{-2}$
0.03	$5.4275(3) \times 10^{-2}$	$-3.3259(2) \times 10^{-2}$	$5.428097 \times 10^{-2}$	$-3.326218 \times 10^{-2}$
		$Z = 10, R_{\text{rms}} = 3.0055$ fm		
0.005	1.2815660(1)	$-2.7991(2) \times 10^{-4}$	1.293808	$-2.864697 \times 10^{-4}$
0.01	2.0994469(3)	$-1.615696(7) \times 10^{-1}$	2.110544	$-1.6396395 \times 10^{-1}$
0.02	3.58815(4)	-1.53364(3)	3.601573	-1.5446311
0.03	5.4099(3)	-3.3070(2)	5.428097	-3.326218
		$Z = 18, R_{\text{rms}} = 3.4028$ fm		
0.005	4.0630599(4)	$-9.5876(8) \times 10^{-4}$	4.191937	$-9.281618 \times 10^{-4}$
0.01	6.7209719(7)	$-5.06648(2) \times 10^{-1}$	6.838164	$-5.3124321 \times 10^{-1}$
0.02	$1.15271(1) \times 10^1$	-4.8903(1)	$1.166910 \times 10^1$	-5.0046046
0.03	$1.7398(1) \times 10^1$	$-1.05775(6) \times 10^1$	$1.758704 \times 10^1$	$-1.077695 \times 10^1$
		$Z = 36, R_{\text{rms}} = 4.1835$ fm		
0.005	$1.4683176(1) \times 10^1$	$-1.09265(4) \times 10^{-2}$	$1.676775 \times 10^1$	$-3.712647 \times 10^{-3}$
0.01	$2.54275429(5) \times 10^1$	-1.769986(7)	$2.735265 \times 10^1$	-2.1249728
0.02	$4.43478(5) \times 10^1$	$-1.82393(3) \times 10^1$	$4.667638 \times 10^1$	$-2.0018418 \times 10^1$
0.03	$6.7277(3) \times 10^1$	$-3.9986(2) \times 10^1$	$7.034814 \times 10^1$	$-4.310779 \times 10^1$
		$Z = 54, R_{\text{rms}} = 4.7964$ fm		
0.005	$2.7057912(3) \times 10^1$	$-9.53525(9) \times 10^{-2}$	$3.772743 \times 10^1$	$-8.353456 \times 10^{-3}$
0.01	$5.1356073(9) \times 10^1$	-3.343263(8)	$6.154347 \times 10^1$	-4.7811889
0.02	$9.27424(9) \times 10^1$	$-3.64837(3) \times 10^1$	$1.050219 \times 10^2$	$-4.5041442 \times 10^1$
0.03	$1.42198(4) \times 10^2$	$-8.1759(4) \times 10^1$	$1.582833 \times 10^2$	$-9.699252 \times 10^1$
		$Z = 82, R_{\text{rms}} = 5.5012$ fm		
0.005	$3.1618260(7) \times 10^1$	$-7.69521(3) \times 10^{-1}$	$8.699562 \times 10^1$	$-1.926222 \times 10^{-2}$
0.01	$8.194625(2) \times 10^1$	-8.91994(2)	$1.419130 \times 10^2$	$-1.1024936 \times 10^1$
0.02	$1.69924(1) \times 10^2$	$-6.55436(4) \times 10^1$	$2.421697 \times 10^2$	$-1.0386099 \times 10^2$
0.03	$2.71469(1) \times 10^2$	$-1.51054(7) \times 10^2$	$3.649853 \times 10^2$	$-2.236549 \times 10^2$

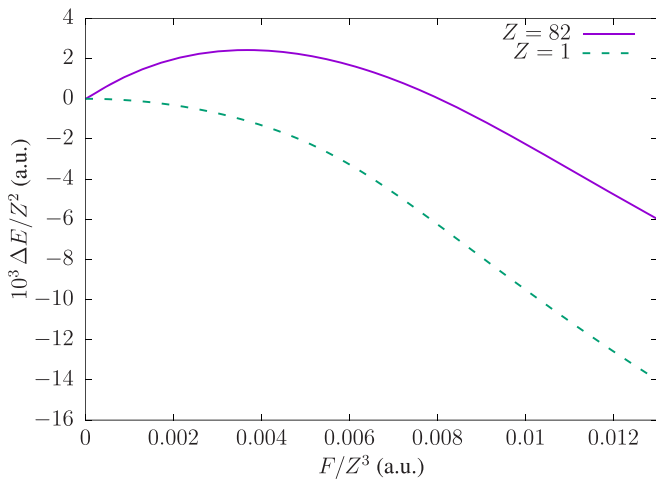


FIG. 5. Stark shift  $\Delta E$  for the  $2s$  state of the hydrogenlike ion with the nuclear charge  $Z$  in the presence of a uniform electric field  $F$ .

parts. There is a more complicated situation for the  $2s$  state. As can be seen from Table IV, for  $Z = 82$  the relativistic and nonrelativistic values have opposite signs. The comparison between results for  $Z = 82$  scaled by  $1/Z^2$  and the corresponding values for  $Z = 1$  is shown in Fig. 5. The difference in behavior is explained by the relativistic effects since for  $Z = 1$  they are almost negligible. It should be noted that the opposite sign for the relativistic value of the Stark shift was previously reported in Ref. [28] for an argon ion.

#### IV. CONCLUSION

In the present work, we calculated the relativistic positions and widths of the Stark resonances in hydrogenlike ions using the complex-scaling method. The calculations were performed for the  $1s$ ,  $2s$ ,  $2p_{1/2}$ , and  $2p_{3/2}$  states of several ions between  $Z = 1$  and 82. The obtained results show the importance of relativistic effects. The comparison between the relativistic and nonrelativistic values leads to the conclusion



that the nonrelativistic calculations are unreliable for heavy ions. The difference is especially drastic for the Stark widths and can be more than one order of magnitude. It is also worth noting that the influence of the relativistic effects is larger for smaller values of the external electric field, which are easier to achieve experimentally.

The performed calculations have confirmed the relativistic suppression of the ground-state width, which was previously shown in Refs. [23,24] using the semiclassical method. In the present work, the existence of the same effect was demonstrated for  $2s$  and  $2p_{1/2}$  states. However, the situation may be the opposite for the  $2p_{3/2}$  state for sufficiently high  $Z$  and weak external field. This emphasizes the importance of relativistic consideration of the Stark effect in heavy ions. It should be noted that despite the fact that the semiclassical theory can provide a qualitatively correct description of the

relativistic effects on the energy width, its quantitative predictions can be quite far from the exact values.

Our consideration was restricted to hydrogenlike ions in the inertial reference frame exposed to a uniform constant electrical field. Real experimental conditions can be much more complicated and include a magnetic field, ion acceleration, and other factors. In order to estimate the influence of all these factors, further development is required. Nevertheless, we expect that the obtained results will be useful for future experiments with heavy partially stripped ions in strong electric fields.

#### ACKNOWLEDGMENT

This work was supported by the BASIS Foundation for the Advancement of Theoretical Physics and Mathematics.

- 
- [1] H. Rausch v. Trautenberg, R. Gebauer, and G. Lewin, *Naturwissenschaften* **18**, 417 (1930).
- [2] R. F. Stebbings, *Science* **193**, 537 (1976).
- [3] M. G. Littman, M. L. Zimmerman, and D. Kleppner, *Phys. Rev. Lett.* **37**, 486 (1976).
- [4] P. M. Koch and D. R. Mariani, *Phys. Rev. Lett.* **46**, 1275 (1981).
- [5] T. Bergeman, C. Harvey, K. B. Butterfield, H. C. Bryant, D. A. Clark, P. A. M. Gram, D. MacArthur, M. Davis, J. B. Donahue, J. Dayton, and W. W. Smith, *Phys. Rev. Lett.* **53**, 775 (1984).
- [6] A. S. Stodolna, A. Rouzée, F. Lépine, S. Cohen, F. Robicheaux, A. Gijbbersen, J. H. Jungmann, C. Bordas, and M. J. J. Vrakking, *Phys. Rev. Lett.* **110**, 213001 (2013).
- [7] M. Hehenberger, H. V. McIntosh, and E. Brändas, *Phys. Rev. A* **10**, 1494 (1974).
- [8] S. A. Zapryagaev, *Opt. Spectrosc.* **44**, 892 (1978).
- [9] L. Benassi and V. Grecchi, *J. Phys. B* **13**, 911 (1980).
- [10] D. Farrelly and W. P. Reinhardt, *J. Phys. B* **16**, 2103 (1983).
- [11] J. A. C. Gallas, H. Walther, and E. Werner, *Phys. Rev. A* **26**, 1775 (1982).
- [12] R. J. Damburg and V. V. Kolosov, *J. Phys. B* **9**, 3149 (1976).
- [13] R. J. Damburg and V. V. Kolosov, *J. Phys. B* **11**, 1921 (1978).
- [14] V. V. Kolosov, *J. Phys. B* **20**, 2359 (1987).
- [15] C. S. Lai, *Phys. Lett. A* **83**, 322 (1981).
- [16] V. V. Kolosov, *J. Phys. B* **16**, 25 (1983).
- [17] A. Maquet, S.-I. Chu, and W. P. Reinhardt, *Phys. Rev. A* **27**, 2946 (1983).
- [18] C. Y. Lin and Y. K. Ho, *J. Phys. B* **44**, 175001 (2011).
- [19] J. Rao, W. Liu, and B. Li, *Phys. Rev. A* **50**, 1916 (1994).
- [20] F. M. Fernández, *Phys. Rev. A* **54**, 1206 (1996).
- [21] U. D. Jentschura, *Phys. Rev. A* **64**, 013403 (2001).
- [22] I. A. Ivanov and Y. K. Ho, *Phys. Rev. A* **69**, 023407 (2004).
- [23] N. Milosevic, V. P. Krainov, and T. Brabec, *Phys. Rev. Lett.* **89**, 193001 (2002).
- [24] N. Milosevic, V. P. Krainov, and T. Brabec, *J. Phys. B* **35**, 3515 (2002).
- [25] V. S. Popov, B. M. Karnakov, and V. D. Mur, *JETP Lett.* **79**, 262 (2004).
- [26] P. A. Batishchev, O. I. Tolstikhin, and T. Morishita, *Phys. Rev. A* **82**, 023416 (2010).
- [27] L. Fernández-Menchero and H. P. Summers, *Phys. Rev. A* **88**, 022509 (2013).
- [28] E. B. Rozenbaum, D. A. Glazov, V. M. Shabaev, K. E. Sosnova, and D. A. Telnov, *Phys. Rev. A* **89**, 012514 (2014).
- [29] F. M. Fernández, *Appl. Math. Comput.* **317**, 101 (2018).
- [30] I. A. Maltsev, D. A. Tumakov, R. V. Popov, and V. M. Shabaev, *Opt. Spectrosc.* **130**, 461 (2022).
- [31] V. Andreev *et al.*, *Nature (London)* **562**, 355 (2018).
- [32] J. W. Blanchard, D. Budker, D. DeMille, M. G. Kozlov, and L. V. Skripnikov, *Phys. Rev. Res.* **5**, 013191 (2023).
- [33] D. Budker, J. R. Crespo López-Urrutia, A. Derevianko, V. V. Flambaum, M. W. Krasny, A. Petrenko, S. Pustelny, A. Surzhykov, V. A. Yerokhin, and M. Zolotarev, *Ann. Phys. (Berlin)* **532**, 2000204 (2020).
- [34] V. A. Zaytsev, I. A. Maltsev, I. I. Tupitsyn, and V. M. Shabaev, *Phys. Rev. A* **100**, 052504 (2019).
- [35] S. Kieslich, S. Schippers, W. Shi, A. Müller, G. Gwinner, M. Schnell, A. Wolf, E. Lindroth, and M. Tokman, *Phys. Rev. A* **70**, 042714 (2004).
- [36] A. Müller, E. Lindroth, S. Bari, A. Borovik, Jr., P.-M. Hillenbrand, K. Holste, P. Indelicato, A. L. D. Kilcoyne, S. Klumpp, M. Martins, J. Viefhaus, P. Wilhelm, and S. Schippers, *Phys. Rev. A* **98**, 033416 (2018).
- [37] V. A. Zaytsev, I. A. Maltsev, I. I. Tupitsyn, V. M. Shabaev, and V. Y. Ivanov, *Opt. Spectrosc.* **128**, 307 (2020).
- [38] E. Ackad and M. Horbatsch, *Phys. Rev. A* **75**, 022508 (2007).
- [39] E. Ackad and M. Horbatsch, *Phys. Rev. A* **76**, 022503 (2007).
- [40] A. Marsman and M. Horbatsch, *Phys. Rev. A* **84**, 032517 (2011).
- [41] I. A. Maltsev, V. M. Shabaev, V. A. Zaytsev, R. V. Popov, and D. A. Tumakov, *Opt. Spectrosc.* **128**, 1100 (2020).
- [42] T.-C. Jagau, *J. Chem. Phys.* **148**, 204102 (2018).
- [43] E. Epifanovsky, *J. Chem. Phys.* **155**, 084801 (2021).
- [44] W. P. Reinhardt, *Annu. Rev. Phys. Chem.* **33**, 223 (1982).
- [45] B. R. Junker, *Adv. At. Mol. Phys.* **18**, 207 (1982).
- [46] Y. K. Ho, *Phys. Rep.* **99**, 1 (1983).
- [47] N. Moiseyev, *Phys. Rep.* **302**, 212 (1998).
- [48] E. Lindroth and L. Argenti, *Adv. Quantum Chem.* **63**, 247 (2012).

- [49] I. A. Maltsev, V. M. Shabaev, R. V. Popov, Y. S. Kozhedub, G. Plunien, X. Ma, and T. Stöhlker, *Phys. Rev. A* **98**, 062709 (2018).
- [50] I. A. Maltsev, V. M. Shabaev, I. I. Tupitsyn, Y. S. Kozhedub, G. Plunien, and T. Stöhlker, *Nucl. Instrum. Methods Phys. Res. Sect. B* **408**, 97 (2017).
- [51] B. Simon, *Phys. Lett. A* **71**, 211 (1979).
- [52] N. Moiseyev and J. O. Hirschfelder, *J. Chem. Phys.* **88**, 1063 (1988).
- [53] U. V. Riss and H. D. Meyer, *J. Phys. B* **26**, 4503 (1993).
- [54] N. Elander and E. Yarevsky, *Phys. Rev. A* **57**, 3119 (1998).
- [55] P. Pirkola and M. Horbatsch, *Phys. Rev. A* **105**, 032814 (2022).
- [56] L. D. Landau and E. M. Lifshitz, *Quantum Mechanics: Non-relativistic Theory* (Pergamon, Oxford, 1977).